BIOCHEMISTRY
including biophysical chemistry & molecular biology

Article

pubs.acs.org/biochemistry

Reconstitution of KCNE1 into Lipid Bilayers: Comparing the Structural, Dynamic, and Activity Differences in Micelle and Vesicle Environments

Aaron T. Coey,[†] Indra D. Sahu,[†] Thusitha S. Gunasekera,[†] Kaylee R. Troxel,[†] Jaclyn M. Hawn,[†] Max S. Swartz,[†] Marilyn R. Wickenheiser,[†] Ro-jay Reid,[†] Richard C. Welch,[‡] Carlos G. Vanoye,[‡] Congbao Kang,[§] Charles R. Sanders,[§] and Gary A. Lorigan*[,†]

[†]Department of Chemistry and Biochemistry, Miami University, Oxford, Ohio 45056, United States

[‡]Division of Genetic Medicine, Department of Medicine, Vanderbilt University, Nashville, Tennessee 37232-2358, United States

[§]Department of Biochemistry and Center for Structural Biology, Vanderbilt University, Nashville, Tennessee 37240, United States

Supporting Information

ABSTRACT: KCNE1 (minK), found in the human heart and cochlea, is a transmembrane protein that modulates the voltage-gated potassium KCNQ1 channel. While KCNE1 has previously been the subject of extensive structural studies in lyso-phospholipid detergent micelles, key observations have yet to be confirmed and refined in lipid bilayers. In this study, a reliable method for reconstituting KCNE1 into lipid bilayer vesicles composed of 1-palmitoyl-2-oleoyl-*sn*-glycero-3-phosphocholine (POPC) and 1-palmitoyl-2-oleoyl-*sn*-glycero-3-phospho(1′-*rac*-glycerol) (sodium salt) (POPG) was developed. Microinjection of the proteoliposomes into *Xenopus* oocytes expressing the human KCNQ1 (K_V7.1) voltage-gated potassium channel led to nativelike modulation of the channel. Circular dichroism spectroscopy demonstrated that the percent helicity of KCNE1 is significantly higher for the protein reconstituted in lipid vesicles than for the previously described structure in 1.0% 1-myristoyl-2-hydroxy-*sn*-glycero-3-phospho(1′-*rac*-glycerol) (sodium salt) (LMPG) micelles. SDSL electron paramagnetic resonance spectroscopic techniques were used to probe the local structure and environment of Ser28, Phe54, Phe57, Leu59, and Ser64 of KCNE1 in both POPC/POPG vesicles and LMPG micelles. Spin-labeled KCNE1 cysteine mutants at Phe54, Phe57, Leu59, and Ser64 were found to be located inside POPC/POPG vesicles, whereas Ser28 was found to be located outside the membrane. Ser64 was shown to be water inaccessible in vesicles but found to be water accessible in LMPG micelle solutions. These results suggest that key components of the micelle-derived structure of KCNE1 extend to the structure of this protein in lipid bilayers but also demonstrate the need to refine this structure using data derived from the bilayer-reconstituted protein to more accurately define its native structure. This work establishes the basis for such future studies.

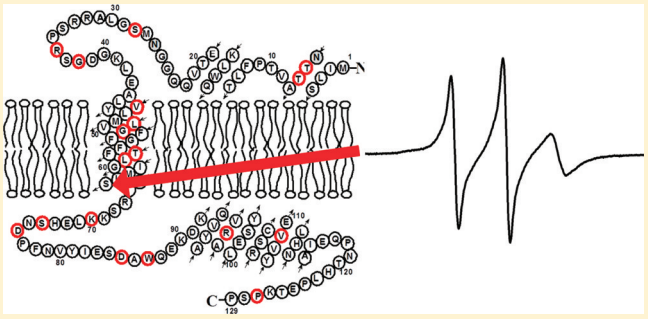

KCNE1 (minK) is a member of the KCNE family of transmembrane proteins that modulate the activity of certain voltage-gated K^+ channels, including KCNQ1 (K_V7.1). KCNE1 forms a complex with KCNQ1 both to slow its voltage-stimulated activation and to enhance its open state conductance, resulting in the I_{Ks} current of the cardiac action potential.[1−3] Hereditary mutations in KCNE1 have been linked to long QT syndrome and deafness.[1,4−8] The structure of KCNE1 was recently determined in LMPG detergent micelles, where its transmembrane domain was observed to be a curved α-helix, with both N- and C-termini consisting of flexibly linked α-helices, some of which have an affinity for the micellar surface.[9] On the basis of this structure and experimentally restrained docking into KCNQ1 channel models, it was hypothesized that KCNE1 interacts with the S4−S5 linker domain of KCNQ1 to restrict the opening of the gate in S6 that generates the delayed channel opening observed in functional studies of KCNQ1 coexpressed with KCNE1.[9−14]

The LMPG micelle environment used in the determination of KCNE1's structure provided a suitable environment for solution NMR experiments because of their isotropic nature. Moreover, the lyso-phospholipid LMPG represents a mild class of detergents that is especially phospholipid-like. However, even the most optimal detergent micelles do not provide a completely natural environment for studies of membrane proteins. This caveat can lead to structural distortions and changes in the stability of both local and global conformations. This means that structures determined in micelles should be

Received: June 16, 2011
Revised: November 4, 2011
Published: November 15, 2011

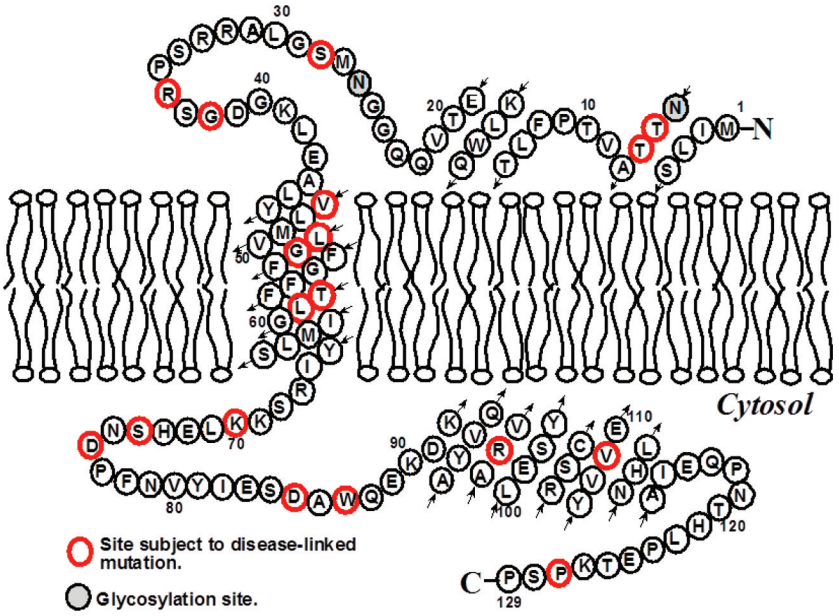

Figure 1. Topological illustration of KCNE1 with respect to a lipid bilayer assuming that the TMD spans residues 46−71 as previously determined for the protein in 7.5% LMPG micelles at 40 °C and pH 6.0.[9−14] The small arrows show the tracing of the peptide chain.

validated by structural measurements taken under conditions in which the protein of interest is reconstituted into vesicles (Figure 1). Moreover, even in cases where the micellar structure captures the key features of the bilayer-associated structure, the micellar structure may require refinement to correct for minor differences such as the exact beginnings and ends of secondary structural elements. In this paper, we describe methods for reconstituting KCNE1 in lipid vesicles and present data that demonstrate that direct structural study of KCNE1 under bilayer conditions is indeed merited for the refinement of the micellar structure to better reflect the actual bilayer structure.

MATERIALS AND METHODS

Site-Directed Mutagenesis. The His tag expression vectors (pET-16b) containing the wild type and a cysteine-less mutant form of KCNE1 [in which its single cysteine residue (105) was mutated to Ala] have been described previously.[9] These vectors were transformed into XL1-Blue *Escherichia coli* cells (Stratagene). Plasmid extracts from these cells were obtained using the QIAprep Spin Miniprep Kit (Qiagen). Site-directed mutagenesis to generate single-cysteine mutants from the Cys-less vector was performed using the QuikChange Lightning Site-Directed Mutagenesis Kit (Stratagene). The KCNE1 mutations were confirmed by DNA sequencing from XL10-Gold *E. coli* (Stratagene) transformants using the T7 primer (Integrated DNA Technologies). Successfully mutated vectors were transformed into BL21-(DE3) CodonPlus-RP *E. coli* cells (Stratagene) for protein overexpression. Mutations S28C and S64C were chosen for EPR measurements to prevent structural perturbations because of the close relationship in structure between serine and cysteine. F54C, F57C, and L59C mutations were chosen as additional sites on the TMD to confirm that the TMD was embedded inside the membrane.

Expression and Purification. A 5 mL preculture of Luria broth containing 50 μg/mL ampicillin was inoculated with the BL21(DE3) KCNE1 transformant of choice. After overnight growth, the preculture was added to 1 L of sterile M9 minimal medium [12.8 g of $Na_2HPO_4{\cdot}7H_2O$, 3.0 g of KH_2PO_4, 0.5 g of NaCl, 1.0 g of NH_4Cl, 0.24 g of $MgSO_4$, 11 mg of $CaCl_2$, 4 g of dextrose, and 50 μg/mL ampicillin (pH 7.0)] and grown in a shaker-incubator at 37 °C and 220 rpm. When the OD_{600} reached 0.8−0.9, protein expression was induced by addition of IPTG to a final concentration of 1 mM, and cultures were allowed to grow overnight at 37 °C.

Cells were collected by centrifugation of cultures. The cell pellets were resuspended in 40 mL of lysis buffer [70 mM Tris-HCl and 300 mM NaCl (pH 8.0)]. After the addition of 0.5 mg of DNase I (bovine pancreas, Fischersci), 1 mg of lysozyme (egg white, Fischer Scientific), 40 μL of RNase A (20 mg/mL, Thermo Scientific), and magnesium acetate to a concentration of 5 mM, the cell lysates were allowed to rotate at 4 °C for 2 h. After rotating, the samples were subjected to sonication for 20 min (5 s on and 5 s off, 10 min total on time, Fisher Scientific Sonic Dismembrator model 500, 40% amplitude). The lysates were centrifuged at 40000*g* for 20 min. The resulting pellet was resuspended in urea buffer [8 M urea, 20 mM Tris-HCl, 150 mM NaCl, 0.2% SDS, and 2 mM β-ME (pH 8.0)] and rotated overnight at room temperature to dissolve the inclusion bodies.

Overnight suspensions were again centrifuged at 40000*g* for 20 min. The resulting supernatant was mixed with 4 mL of Ni-NTA resin (Thermo Scientific) that had been previously equilibrated with urea buffer. Samples were then rotated at room temperature for 2 h. Excess protein was washed away by pouring the resin suspension into a 20 mL gravity flow column and rinsing with 6 volumes of TS/SDS buffer [20 mM Tris-HCl, 200 mM NaCl, 0.2% SDS, and 2 mM β-ME (pH 8.0)]. To produce LMPG micelle samples, 0.1% LMPG was substituted for 0.2% SDS in the TS buffer washes. Purified His-tagged KCNE1 was eluted into five 2 mL fractions using elution buffer [250 mM imidazole, 0.2% SDS, and 2 mM β-ME (pH 7.0)]; 0.1% LMPG was substituted for 0.2% SDS for LMPG micelle samples. The fractions were pooled together and concentrated to a volume of 1.5 mL using a 3.5 kDa molecular mass cutoff spin column (Millipore). The total

concentration was obtained by measuring the OD_{280} and using an extinction coefficient of 1.2 mg/mL per 1.0 absorbance in a 1 cm cell.[15] The purity of the KCNE1 protein was confirmed by sodium dodecyl sulfate−polyacrylamide gel electrophoresis.

MTSL Labeling. An MTSL (Toronto Research Chemicals) stock (250 mM in methanol) was added directly to the concentrated protein in elution buffer at a 10:1 MTSL:protein molar ratio. The solution was allowed to react overnight at room temperature in the dark while being vigorously stirred. The MTSL reaction mixture was loaded into a 3.5 kDa molecular mass cutoff regenerated cellulose dialysis bag (Fisher Scientific) and dialyzed twice against 4 L of phosphate buffer [100 mM NaH_2PO_4 and 0.2% SDS (pH 7.2)] for 24 h each time; 0.1% LMPG was substituted for 0.2% SDS in the case of LMPG micelle samples. After dialysis, the samples were centrifuged at 6000*g* for 5 min to remove any precipitates. The resulting supernatant was used for EPR and CD spectroscopy. This method was found to be most effective for removing excess MTSL while preserving the detergent environment and minimizing protein aggregation.

Reconstitution into Lipid Bilayers. POPC and POPG powdered lipids (Avanti, Alabaster, AL) were dissolved to a final concentration of 5 mM (9:1 POPC:POPG molar ratio) in 100 mM NaH_2PO_4 and 0.5% DOM (pH 7.2) by repeating at least 10 freeze−thaw−sonication cycles until the solutions were clear. SM2 Bio Beads (Bio-Rad) were washed with 8 × 15 mL volumes of methanol followed by 8 × 15 mL volumes of water prior to use. Samples were reconstituted by mixing 1 mL of the lipid slurry with 157 μg of dialyzed MTSL-labeled protein in 0.2% SDS (500:1 lipid:protein molar ratio) and freezing and thawing them twice to equilibrate them. The lipid/protein mixture was then added to 300 mg of wet Bio Beads and rotated at room temperature for 2 h. Previous studies showed that this amount of Bio Beads combined with this concentration of detergent effectively removes all detergent and forms MLVs.[16] The resulting sample was centrifuged at 2000*g* for 5 min to remove Bio Beads. The supernatant was concentrated by ultracentrifugation at 300000*g* for 30 min. The proteoliposome pellet was thoroughly resuspended in 50 μL of 100 mM NaH_2PO_4 (pH 7.2) and immediately used in spectroscopic studies. The resulting sample was white, opaque, and highly viscous.

CW EPR Spectroscopy. CW EPR spectroscopy was conducted on a Bruker EMX X-band spectrometer. Spectra were recorded over a scan width of 100 G with a field modulation of 1 G at a frequency of 100 kHz. Samples were placed in a glass capillary tube and had a volume of 50 μL and a total protein concentration of approximately 200 μM for micelle samples and 50 μM for proteoliposomes. Each sample was scanned 10−20 times with a microwave intensity of 10 mW at 298 K.

CW EPR Power Saturation Studies. Insertion of KCNE1 into POPC/POPG bilayers was verified using CW EPR power saturation at X-band. Power saturation experiments were performed on a Bruker EMX X-band CW EPR spectrometer consisting of an ER 041XG microwave bridge coupled with an ER 4123D CW resonator (Bruker BioSpin). Samples were loaded into gas permeable TPX capillary tubes with a total volume of 3−4 μL at a concentration of 30−50 μM. EPR data were collected using a modulation amplitude of 1 G and varying microwave power of 0.4−100 mW. The scan range of all spectra was 100 G, and the final spectra were obtained by signal averaging 10 scans. The power saturation method works on the principle that under nonsaturating conditions, the height of the spectral lines is linearly proportional to the square root of the incident microwave power, $P_{1/2}$.[17] If the microwave power is subsequently increased, the increase in signal amplitude becomes less linear with $P_{1/2}$, and signal height starts to decrease as the sample saturates.

Nitrogen is used as a control to purge the sample of oxygen and other paramagnetic relaxing agents. The power saturation curves were obtained for the S28C (probe outside of the model membrane) and F54C, F57C, L59C, and S64C (probe inside) sites on KCNE1 under three conditions: (1) equilibrated with nitrogen as a control, (2) equilibrated with lipid-soluble paramagnetic reagent 20% oxygen (air), and (3) equilibrated with nitrogen in the presence of a water-soluble paramagnetic reagent, NiEDDA (1 mM), as previously synthesized.[18] The samples were purged with gas for at least 60 min at a rate of 10 mL/min before each measurement was taken. High-purity nitrogen and house supply compressed air lines were used during the experiments. The resonator remained connected to the gas during all measurements, and the sample temperature was held at 298 K. The peak-to-peak amplitude of the first-derivative $m_I = 0$ resonance line (A) was measured and plotted versus the square root of the incident microwave power. The data points were then fit using a Matlab software script according to eq 1:

$$A = I\sqrt{P}[1 + (2^{1/\varepsilon} - 1)P/P_{1/2}]^{-\varepsilon} \quad (1)$$

where I is a scaling factor, $P_{1/2}$ is the power at which the first-derivative amplitude is reduced to half of its unsaturated value, and ε is a measure of the homogeneity of saturation of the resonance line. In eq 1, I, ε, and $P_{1/2}$ are adjustable parameters and yield a characteristic $P_{1/2}$ value. The corresponding Φ depth parameters were calculated.[17,19−21] The membrane depth (angstroms) of each spin-labeled KCNE1 mutant was calculated according to eq 2:

$$\text{depth} = 5.6\Phi + 2.3 \quad (2)$$

The bilayer depth calibration equation (eq 2) was determined using vesicles incorporating standard *n*-doxyl-labeled POPCs (Avanti Polar Lipids) containing unlabeled wild-type (WT) KCNE1. Depth parameters (Φ) were measured and plotted versus known depths for each labeled POPC.[17,22,23] A linear dependence of Φ was found for the PCSLs, and eq 2 was derived via linear regression analysis.

Functional Analysis of KCNQ1 and KCNE1. Complementary DNAs (cDNAs) encoding KCNQ1 and KCNE1 were constructed in plasmid vectors pSP64T and pRc/CMV, respectively, as previously described.[24] All constructs were verified by sequencing. cRNA was transcribed in vitro from *Eco*RI (pSP64T-KCNQ1) or *Xba*I (pRc/CMV-KCNE1) digested linear DNA templates using Sp6 or T7 RNA polymerase and the mMessage mMachine transcription system (Ambion Inc., Austin, TX). The size and integrity of cRNA preparations were evaluated by formaldehyde−agarose gel electrophoresis, and full-length cRNA concentrations were estimated by comparison with a 0.24−9.5 kb RNA ladder (Sigma, St. Louis, MO).

Female *Xenopus laevis* were anesthetized by immersion in 0.2% tricaine for 15−30 min. Ovarian lobes were removed, and oocytes were manually defolliculated. Stage V−VI oocytes were injected with 25 nL of cRNA (KCNQ1, 6 ng/oocyte; KCNE1 constructs, 3 ng/oocyte) and incubated at 18 °C for 48−96 h in

L-15 (Leibovitz's medium, Invitrogen, Carlsbad, CA) diluted 1:1 with water and supplemented with penicillin (150 units/mL) and streptomycin (150 μg/mL). Some oocytes were injected with 25 nL of water as a control for endogenous currents. Because previous studies revealed that *Xenopus* oocytes express endogenous KCNE genes,[25] currents from oocytes injected with KCNQ1 cRNA alone were always recorded from representative oocytes in each batch to test for endogenous KCNEs.

Incorporation of Recombinant His-KCNE1 Protein into *Xenopus* Oocytes. Our previous studies demonstrated that, following microinjection into oocytes, purified KCNE1 protein solubilized in LMPG micelles is incorporated into the plasma membrane, where it modulates exogenous human KCNQ1 expressed therein.[9−14] In this study, a similar protocol was employed, but with KCNE1 in POPC/POPG vesicles at a protein concentration of 2.5 mg/mL. Vesicle samples were successfully prepared by removal of detergent through either dialysis or Bio Beads. The oocytes were first injected with KCNQ1 cRNA, followed by injection of 25 nL of protein-containing or protein-free liposomes 24 h later.

Electrophysiological Analysis. Oocyte membrane currents were recorded at room temperature 2 days after injection using a two-microelectrode voltage-clamp technique with an OC-725B amplifier (Warner Instruments Corp., Hamden, CT). Oocytes were bathed at room temperature in a modified ND96 solution containing 96 mM NaCl, 4 mM KCl, 2 mM $MgCl_2$, 0.1 mM $CaCl_2$, and 5 mM HEPES (pH 7.6) (~200 mosm/kg). Data were recorded using Clampex 7 (Molecular Devices Corp., Sunnyvale, CA), filtered at 500 Hz, and digitized at 2 kHz. Data were analyzed and plotted using a combination of Clampex, SigmaPlot 2000 (SPSS Science, Chicago, IL), and Origin 7.0 (OriginLab, Northampton, MA). Current−voltage and normalized isochronal voltage−activation relationships were obtained by measuring current at 2 s during depolarizing pulses between −50 and 60 mV from a holding potential of −80 mV. The normalized isochronal data were fit with a Boltzmann function of the form $1/\{1 + \exp[(V - V_{1/2})/k_v]\}$, where $V_{1/2}$ is the half-maximal activation voltage and k_v is the slope factor. Oocytes with currents −80 mV (holding potential) larger than currents measured for water-treated oocytes (−0.15 μA) were considered leaky and not used for analysis.

CD Spectroscopy. CD experiments were performed on a Jasco model J-810 spectropolarimeter over a wavelength range of 190−250 nm. Each sample was prepared in triplicate. Samples were subjected to 10 scans with a step size of 1 nm. The cuvette path length was 1.00 mm, and spectra were recorded at 298 K. Instrument calibration was performed with a standard solution of *d*-(+)-10-camphorsulfonic acid. Protein concentrations were held at 15 μM as confirmed by a BCA assay (Thermo Scientific). When necessary, samples were diluted in 100 mM NaH_2PO_4 (pH 7.2). Scattering effects produced by the sample matrix were found to be reduced when the vesicle samples were passed through a 100 nm pore size extruder.

CD Spectral Simulations. CD spectral simulations were performed using the DICHROWEB website (http://dichroweb.cryst.bbk.ac.uk) that was supported by grants to the BBSRC Centre for Protein and Membrane Structure and Dynamics (CPMSD).[26] The Contin-LL algorithm with reference set 4 and a spectral width of 190−240 nm was used for all simulations.[27−29] All CD and EPR data were plotted using Igor (Wavemetrics, Tigard, OR).

RESULTS

Homogeneous Reconstitution of KCNE1 in Bilayered Lipid Vesicles. POPC/POPG vesicles were chosen as the bilayer model membrane system in which to solubilize KCNE1. These two lipids are fully miscible, are akin to the most common phospholipids found in mammalian cell membranes, and have phase transition temperatures to the L_α liquid crystalline phase of <0 °C. The POPC:POPG molar ratio was set at 9:1 to mimic the 10−20 mol % of anionic phospholipids typically found in mammalian membranes.[30]

Several reconstitution methods were tried, including dialysis from aqueous SDS detergent into POPC/POPG vesicles and removal of detergent by size exclusion chromatography. The dialysis method led to extensive sample aggregation, while size exclusion chromatography proved to be inconsistent in sample preparation. Reconstitution using SM2 Bio Beads proved to be the most efficient and consistent for reliable sample reproduction. Interestingly, samples produced using dialysis still showed proper channel modulation upon injection into oocytes.

Figure 2 shows X-band CW EPR spectra of spin-labeled S28C and S64C KCNE1 in 1% LMPG micelles and in POPC/POPG liposomes (pH 7.2). Inspection of the data reveals a broadening in the spectral line widths when moving from the micelles to the lipid bilayer and that residue S28C is more mobile than residue S64C in a lipid bilayer. This indicates that the dynamic motion of the nitroxide spin-label is slower in the membrane environment than in the micelles and that resides within the membrane are less mobile than those outside. Similar line broadening has previously been reported.[22,31−33]

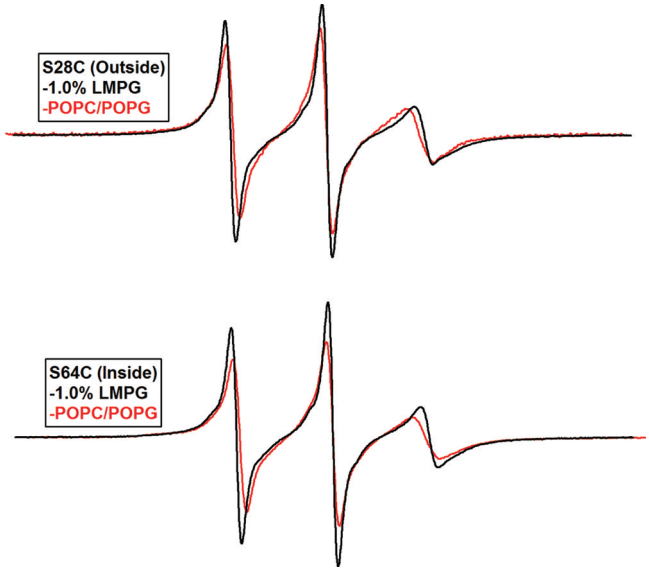

Figure 2. CW EPR (X-band) spectra of KCNE1 mutants S28C (top) and S64C (bottom): black for 1.0% LMPG micelles and red for 9:1 POPC/POPG proteoliposomes (500:1 lipid:protein). For all samples, the pH was 7.2 and the temperature was 298 K. Spectra were normalized by spin concentration to show the difference in dynamic properties between S28C and S64C in a bilayer as compared to LMPG micelles.

Microinjection of Bilayer-Reconstituted KCNE1 into KCNQ1 Channel Expression Oocytes. The ability of KCNE1 to associate with and modulate human KCNQ1 that was exogenously expressed in *Xenopus* oocytes was preserved

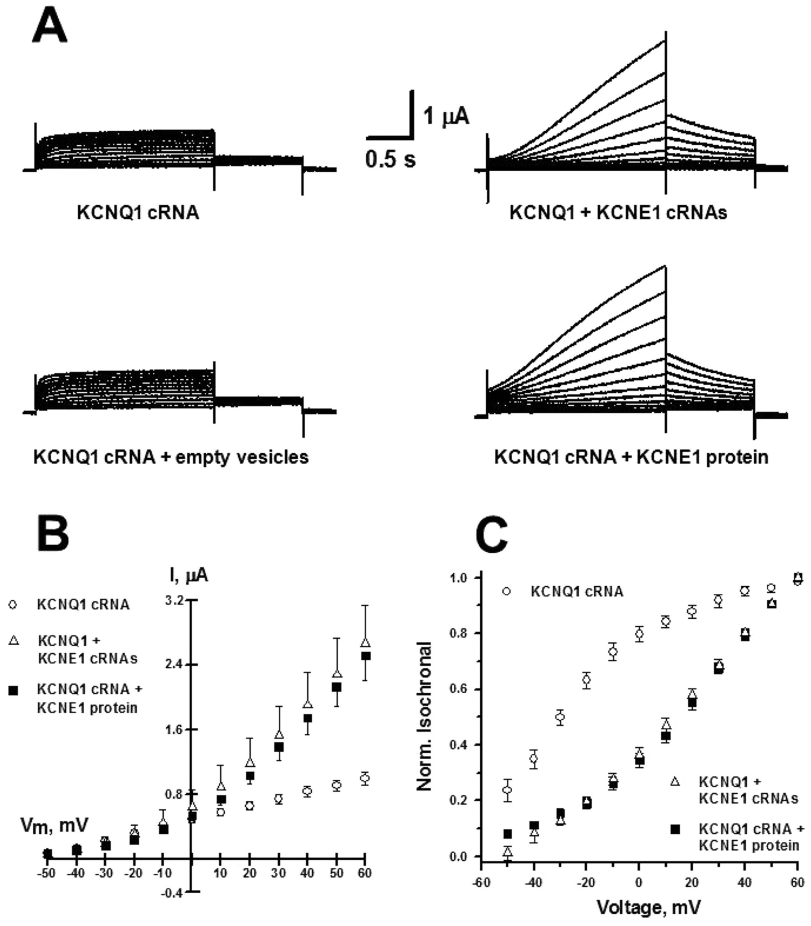

Figure 3. Functional expression of KCNE1 protein in *Xenopus* oocytes. (A) Representative current traces recorded from oocytes injected with KCNQ1 cRNA, KCNQ1 and KCNE1 cRNAs, KCNQ1 cRNA and empty vesicles, and KCNQ1 cRNA and KCNE1 protein in lipid vesicles. (B) Current−voltage relationship for currents measured after 2 s test pulses from a holding potential of −80 mV for oocytes injected with KCNQ1 cRNA (○; n = 10), KCNQ1 and KCNE1 cRNA (△; n = 12), and KCNQ1 cRNA and KCNE1 protein in lipid vesicles (■; n = 12). (C) Normalized isochronal activation curves for oocytes. Data were fit with a Boltzmann function and resulted in the following fit parameters: for KCNQ1 cRNA (○), $V_{1/2}$ = −32.5 ± 3.0 and k_V = 20.4 ± 2.4; for KCNQ1 and KCNE1 cRNAs (△), $V_{1/2}$ = 28.8 ± 0.6 and k_V = 20.6 ± 0.7; and for KCNQ1 cRNA and KCNE1 protein in lipid vesicles (■), $V_{1/2}$ = 34.1 ± 1.3 and k_V = 23.9 ± 1.1.

when KCNE1 in POPC/POPG vesicles was microinjected into oocytes. The characteristic delayed channel opening resulting from KCNQ1−KCNE1 coassembly was observed and was similar for both microinjected recombinant protein and KCNE1 that was expressed in the oocytes following KCNE1 cRNA injection (Figure 3).[15] A negative control experiment in which protein-free POPC/POPG vesicles were injected did not result in modulation of KCNQ1 channel function, as expected. This indicates that KCNE1 in POPC/POPG vesicles was somehow transferred into the oocyte membranes, perhaps by fusion of the vesicles with the native membranes, to yield a properly functioning channel complex at the plasma membrane.

Probing the Topology of KCNE1 Using Power Saturation EPR. Power Saturation EPR experiments were conducted with KCNE1 to examine the location of and insertion of different residues with respect to the membrane (Figure 4). KCNE1 samples in LMPG micelles and POPC/POPG vesicles were analyzed under conditions in which samples were exposed to NiEDDA, N_2, or air (which contains O_2). NiEDDA is highly polar and resides mostly in the aqueous phase. Conversely, paramagnetic O_2 is nonpolar and resides mostly within the hydrophobic lipid bilayer. Because NiEDDA and O_2 function as paramagnetic relaxing agents that decrease the T_1 of the unpaired electron in the nitroxide spin-label, the relative location of an MTSL spin-label with respect to the aqueous phase and the membrane can be determined by examining signal intensity as a function of microwave power.

Figure 4 reveals that the addition of NiEDDA to S28C KCNE1 has a dramatic effect on the power saturation curve in both LMPG micelles and POPC/POPG vesicles. This indicates that S28C is water accessible in both matrices. Inspection of the power saturation profile of KCNE1 S64C (Figure 4) indicates that O_2 in air alters the relaxation profile much more than both N_2 and NiEDDA in POPC/POPG vesicles but not in LMPG micelles,[9] demonstrating that position 64 is buried inside the hydrophobic vesicle membrane but water accessible in LMPG micelles. The N_2 control experiments showed similar saturation results for both mutants. Both S28C and S64C are water-exposed in LMPG micelles, but their water access diverges upon reconstitution into lipid vesicles where S28C remains water-exposed but S64C appears to be buried in a water inaccessible part of the bilayer.

Additional CW EPR power saturation experiments (see the Supporting Information) and depth parameter calculations were conducted on additional mutants (F54C, F57C, and L59C) to confirm that KCNE1 has a transmembrane domain.

dx.doi.org/10.1021/bi2009294 | *Biochemistry* 2011, 50, 10851−10859

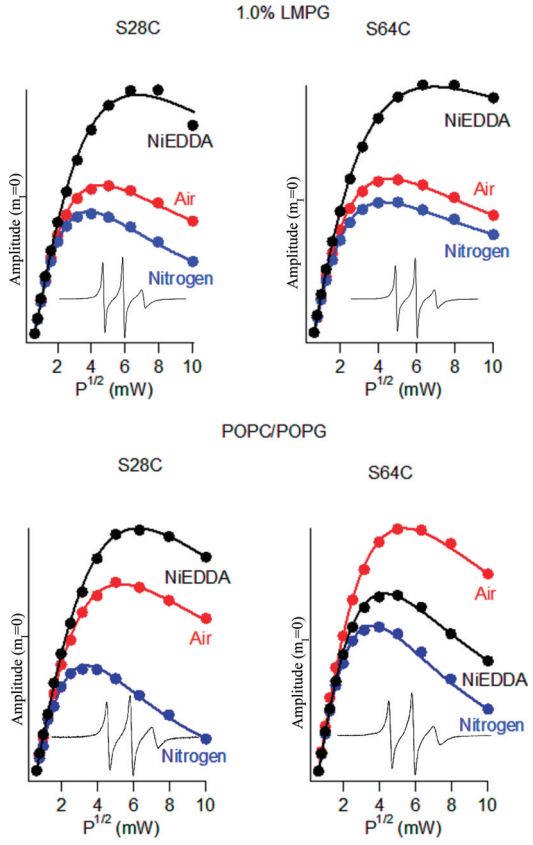

Figure 4. EPR power saturation curves for KCNE1 in 1% LMPG micelles and POPC/POPG vesicles at pH 7.2 and 298 K. Mutation S28C is outside the lipid bilayer, and mutation S64C is part of the transmembrane domain.

The power saturation results for these mutants are similar to those for S64C. Table 1 shows the calculated depth parameter (Φ) values and membrane depth from the power saturation experiments. Mutants F54C, F57C, L59C, and S64C follow a trend as the depth parameter (Φ) increases from 0.8 to 1.9 and then decreases again to 1.1, indicating that the predicted TMD is correctly spanning the membrane (Figure 1). Mutation L59C has the largest Φ value and is located near the center of the membrane, while mutants F54C, F57C, and S64C have lower Φ values indicating that they are within the membrane, but not as deep. S28C has a negative Φ value indicating it resides outside of the membrane in the aqueous phase.[17,20,21]

Table 1. Depth Parameter Values (Φ) and Membrane Depths for Different Spin-Labeled KCNE1 Residues in POPC/POPG Vesicles[a]

label position	depth parameter (Φ)	depth (Å)
S28C	−1.0	
F54C	0.8	6.8
F57C	1.4	10.1
L59C	1.9	12.9
S64C	1.1	8.5

[a]An increase in Φ indicates that a residue is buried more deeply in the membrane. Negative Φ values indicate that a residue is not associated with the membrane.

A calibration curve based on known locations of *n*-doxyl POPCs was established for our membrane protein samples. WT (unlabeled) KCNE1 was incorporated into each of the spin-labeled lipid samples in the same manner as the labeled protein.[17,22] The Φ values for n = 5, 7, and 10 doxyl-POPC, along with published depths for each PCSL, were used to calculate distances into the membrane for each KCNE1 mutant.[23] On the basis of the solution NMR structure of KCNE1 in LMPG micelles, residue G60 should be at or near the center of the membrane bilayer.[15] If we take into account the fact that each residue is approximately 1.5 Å in depth from the next residue, this calibration of distance indicates that the center of our membrane system (POPC/POPG) is approximately 15 Å.[17] The errors in these measurements are approximately ±2 Å because of the uncertainty introduced into the measurement of the depth parameter (Φ). This value is consistent with the length of the TMD of KCNE1 from the published solution NMR structure.[15] Similar trends in Φ values and overall membrane thickness have been observed in the literature for transmembrane proteins.[22,34]

Secondary Structure Content in Phospholipid Vesicles versus Micelles. Figure 5 shows CD spectra of WT KCNE1 in 1.0% LMPG micelles and in POPC/POPG vesicles at pH 7.2 and 298 K. CD spectroscopy of WT KCNE1 showed a predominately α-helical pattern in both micelle and lipid bilayer environments. Spectra recorded in LMPG and POPC/POPG vesicles show similar α-helical contents as indicated by the peak at 195 nm and troughs at 208 and 222 nm. KCNE1 in 1.0% LMPG was found to have 44% helical content, in good agreement with the value of 43% as determined in the NMR-based structural analysis that was conducted at pH 6.0 and 313 K.[9] An increase in α-helical content to 60% was observed when the sample moved from a micelle environment to POPC/POPG vesicles as indicated by an increase in the height of the peak at 195 nm and depth of the troughs at 208 and 222 nm. The CD data clearly indicate that KCNE1 forms a more ordered structure upon insertion into a lipid bilayer with a higher α-helical content.

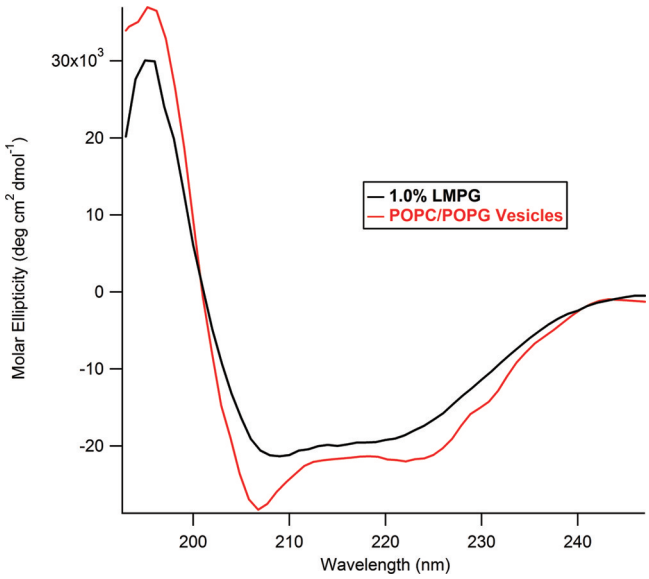

Figure 5. CD spectra of WT KCNE1 in micelle and vesicle environments: black for 1.0% LMPG micelles with 15 μM WT KCNE1 at pH 7.2 and 298 K and red for POPC/POPG MLVs at a 500:1 lipid:protein ratio with WT KCNE1 at pH 7.2 and 298 K.

dx.doi.org/10.1021/bi2009294 | *Biochemistry* 2011, 50, 10851–10859

DISCUSSION

Previous structural studies of KCNE1 were conducted in 7.5% LMPG micelles at pH 6.0 and 313 K, a medium that is believed to be relatively nativelike in terms of its ability to support the native stability, structure, and functionality of membrane proteins. However, even the best micelles are an imperfect mimic of actual lipid bilayers, such that it is imperative to test key features of the micelle-derived structure of KCNE1 for extrapolation to bilayered membrane conditions. For example, the transmembrane helix of KCNE1 was found to be curved in LMPG micelles, an observation that figures prominently in a structural detailed working model for KCNE1 modulation of KCNQ1.[9] Is that curvature truly present in actual lipid bilayers, or is it a micellar artifact? To cite a second example, the transmembrane helix of KCNE1 in micelles extends from residue 46 to 71.[9] It is important to test whether in the more ordered matrix of lipid bilayers the transmembrane domain helix extends beyond the limits observed in micelles. The reconstitution in this work of KCNE1 in POPC/POPG vesicles combined with data that demonstrate the feasibility of conducting site-directed spin labeling EPR spectroscopic measurements set the stage for a rigorous testing and refinement of the KCNE1 structure in a bilayer environment.

The fact that POPG/POPC vesicles represent a suitable model membrane composition for studying the structure of KCNE1 is at least partially validated by the fact that injection of recombinant vesicle-reconstituted KCNE1 into oocytes led to the delivery of KCNE1 to the oocyte membranes where KCNE1 was able to coassemble with the KCNQ1 potassium channel and modulate its function in a nativelike fashion. Similar results were previously obtained when KCNE1 in LMPG micelles was injected into oocytes.[15] Given that we have confirmed that KCNE1 is largely helical in the vesicles, it is very unlikely that its secondary structure would be dramatically altered during the transfer of the protein from the vesicles to the oocyte membranes. This suggests that KCNQ1 associates with the mostly helical form of KCNE1, not a β-sheet-dominated structure as was previously seen for a peptide corresponding to the TMD of KCNE1 following reconstitution of this peptide into vesicles by cosolubilization of the peptide with lipid in an organic solvent and then removal of the solvent via dialysis in an aqueous reservoir.[35]

Previous work suggests that the method used when incorporating KCNE1 into a lipid bilayer is crucial to determining what type of secondary structure the protein adopts.[36,37] The TMD of KCNE1 is very hydrophobic and has several polar residues on either end. It was hypothesized that these polar residues are responsible for anchoring the protein to the polar membrane surface while the inner nonpolar residues interact with the lipid carbon chains. This amphipathic nature makes KCNE1 very insoluble and prone to aggregation in aqueous solution where it adopts a primarily β-sheet conformation. Membrane reconstitution based on selective removal of detergent from mixed detergent/lipid micelle samples using SM Bio Beads, as employed here, keeps KCNE1 in contact with high concentrations of either detergent or lipids at all times to avoid contact with other proteins and prevent aggregation. The lipid:protein molar ratio is also significantly higher (500:1) than those in previous studies in which lipid:protein ratios as low as 7.8:1 led to the formation of β-sheets in a peptide version of the TMD.[35]

Having established methods for reconstituting both WT and spin-labeled mutant forms of KCNE1 and verifying structural and functional integrity, we also conducted preliminary EPR and CD spectroscopic experiments that not only set the stage for future more extensive studies of KCNE1's bilayer-associated structure and dynamics but also provide some interesting comparisons of its properties in bilayer vesicles versus mild detergent (LMPG) micelles. In particular, we observed that LMPG micelles do not completely mimic the natural environment of a lipid bilayer as indicated by CW EPR power saturation data. Residue S64C, previously shown to reside inside an LMPG micelle, is still water accessible in the micelle but not in a vesicle bilayer, likely because of the water permeable nature of the micelle. S28C and S64C are thus indistinguishable in LMPG micelles with respect to their water accessibility. It may prove that S64C still sits at a similar depth in the membrane compared to the micelles but is simply more water accessible in micelles.

As mentioned previously, the LMPG structure of KCNE1 shows several peripheral α-helices that are docked into the micelle at specific residues.[9] CW power saturation EPR will prove to be an invaluable technique in confirming these docking sites in lipid bilayers. EPR spectroscopy will also be used to fully explore the TMD of KCNE1 and determine which residues span this region in POPC/POPG vesicles as compared to LMPG micelles. Recent structure–function studies suggest that an amphipathic helix located just after the TMD may sit on the membrane surface.[38,39] Considering this helix, the ability of the bilayer to stabilize α-helical structures, and the many helical segments that exist in the previous LMPG micelle structure, we find it easy to see how a bilayer could function to stabilize and extend these helical segments, giving rise to a helical content higher than that previously reported in micelles.[9] Our future work will also seek to determine where the additional α-helical content arises as discovered through CD spectroscopy using the wide array of techniques EPR spectroscopy offers for studying membrane protein structure.

ASSOCIATED CONTENT

Supporting Information

CW EPR and power saturation data for KCNE1 residues F54C, F57C, and L59C in POPC/POPG vesicles. This material is available free of charge via the Internet at http://pubs.acs.org.

AUTHOR INFORMATION

Corresponding Author

*Telephone: (513) 529-2813. Fax: (513) 529-5715. E-mail: lorigag@muohio.edu.

Funding

This work was generously supported by National Institutes of Health Grants RO1 GM60259-01 (to G.A.L.) and RO1 DC007416 (to C.R.S.). Funding was also provided by National Science Foundation (NSF) Grant CHE-1011909 (to G.A.L.) and the NSF REU (CHE1004875) program.

ACKNOWLEDGMENTS

We greatly appreciate the EPR expertise of Dr. Robert M. McCarrick of the Miami University Department of Chemistry and Biochemistry, and we thank Dr. Amanda C. Dabney-Smith of the Miami University Department of Chemistry and Biochemistry for her extensive knowledge and advice in molecular biology.

■ ABBREVIATIONS

β-ME, 2-mercaptoethanol; CD, circular dichroism; CMC, critical micelle concentration; CW, continuous wave; DEER, double electron−electron resonance; DOM, *n*-dodecyl β-D-maltoside; DPC, dodecylphosphatidylcholine; EPR, electron paramagnetic resonance; IPTG, isopropyl β-D-thiogalactopyranoside; LMPG, 1-myristoyl-2-hydroxy-*sn*-glycero-3-phospho(1′-*rac*-glycerol) (sodium salt); LUV, large unilamellar vesicle; MLV, multilamellar vesicle; MTSL, *S*-(2,2,5,5-tetramethyl-2,5-dihydro-1*H*-pyrrol-3-yl)methyl methanesulfonothioate; NiEDDA, nickel(II) ethylenediaminediacetate; POPC, 1-palmitoyl-2-oleoyl-*sn*-glycero-3-phosphocholine; POPG, 1-palmitoyl-2-oleoyl-*sn*-glycero-3-phospho(1′-*rac*-glycerol) (sodium salt); SDS, sodium dodecyl sulfate; TMD, transmembrane domain; WT, wild type.

■ REFERENCES

(1) Barhanin, J., Lesage, F., Guillemare, E., Fink, M., Lazdunski, M., and Romey, G. (1996) K(V)LQT1 and lsK (minK) proteins associate to form the I(Ks) cardiac potassium current. *Nature 384*, 78−80.

(2) Sanguinetti, M. C., Curran, M. E., Zou, A., Shen, J., Spector, P. S., Atkinson, D. L., and Keating, M. T. (1996) Coassembly of K(V)LQT1 and minK (IsK) proteins to form cardiac I(Ks) potassium channel. *Nature 384*, 80−83.

(3) McCrossan, Z. A., and Abbott, G. W. (2004) The MinK-related peptides. *Neuropharmacology 47*, 787−821.

(4) Abbott, G. W., and Goldstein, S. A. (2002) Disease-associated mutations in KCNE potassium channel subunits (MiRPs) reveal promiscuous disruption of multiple currents and conservation of mechanism. *FASEB J. 16*, 390−400.

(5) Chen, Y. H., Xu, S. J., Bendahhou, S., Wang, X. L., Wang, Y., Xu, W. Y., Jin, H. W., Sun, H., Su, X. Y., Zhuang, Q. N., Yang, Y. Q., Li, Y. B., Liu, Y., Xu, H. J., Li, X. F., Ma, N., Mou, C. P., Chen, Z., Barhanin, J., and Huang, W. (2003) KCNQ1 gain-of-function mutation in familial atrial fibrillation. *Science 299*, 251−254.

(6) Jespersen, T., Grunnet, M., and Olesen, S. P. (2005) The KCNQ1 potassium channel: From gene to physiological function. *Physiology 20*, 408−416.

(7) Peters, T. A., Monnens, L. A., Cremers, C. W., and Curfs, J. H. (2004) Genetic disorders of transporters/channels in the inner ear and their relation to the kidney. *Pediatr. Nephrol. 19*, 1194−1201.

(8) Splawski, I., Tristani-Firouzi, M., Lehmann, M. H., Sanguinetti, M. C., and Keating, M. T. (1997) Mutations in the hminK gene cause long QT syndrome and suppress IKs function. *Nat. Genet. 17*, 338−340.

(9) Kang, C., Tian, C., Sonnichsen, F. D., Smith, J. A., Meiler, J., George, A. L. Jr., Vanoye, C. G., Kim, H. J., and Sanders, C. R. (2008) Structure of KCNE1 and implications for how it modulates the KCNQ1 potassium channel. *Biochemistry 47*, 7999−8006.

(10) Panaghie, G., Tai, K. K., and Abbott, G. W. (2006) Interaction of KCNE subunits with the KCNQ1 K^+ channel pore. *J. Physiol. 570*, 455−467.

(11) Melman, Y. F., Krumerman, A., and McDonald, T. V. (2002) A single transmembrane site in the KCNE-encoded proteins controls the specificity of KvLQT1 channel gating. *J. Biol. Chem. 277*, 25187−25194.

(12) Melman, Y. F., Um, S. Y., Krumerman, A., Kagan, A., and McDonald, T. V. (2004) KCNE1 binds to the KCNQ1 pore to regulate potassium channel activity. *Neuron 42*, 927−937.

(13) Yarov-Yarovoy, V., Baker, D., and Catterall, W. A. (2006) Voltage sensor conformations in the open and closed states in ROSETTA structural models of K^+ channels. *Proc. Natl. Acad. Sci. U.S.A. 103*, 7292−7297.

(14) Panaghie, G., and Abbott, G. W. (2007) The role of S4 charges in voltage-dependent and voltage-independent KCNQ1 potassium channel complexes. *J. Gen. Physiol. 129*, 121−133.

(15) Tian, C., Vanoye, C. G., Kang, C., Welch, R. C., Kim, H. J., George, A. L. Jr., and Sanders, C. R. (2007) Preparation, functional characterization, and NMR studies of human KCNE1, a voltage-gated potassium channel accessory subunit associated with deafness and long QT syndrome. *Biochemistry 46*, 11459−11472.

(16) Lambert, O., Levy, D., Ranck, J. L., Leblanc, G., and Rigaud, J. L. (1998) A new "gel-like" phase in dodecyl maltoside-lipid mixtures: Implications in solubilization and reconstitution studies. *Biophys. J. 74*, 918−930.

(17) Altenbach, C., Greenhalgh, D. A., Khorana, H. G., and Hubbell, W. L. (1994) A collision gradient method to determine the immersion depth of nitroxides in lipid bilayers: Application to spin-labeled mutants of bacteriorhodopsin. *Proc. Natl. Acad. Sci. U.S.A. 91*, 1667−1671.

(18) Averill, D. F., Legg, J. I., and Smith, D. L. (1972) 5-Coordinate, Square-Pyramidal Chelate Complexes of a Novel Tetradentate Amino-Acid Like Ligand. *Inorg. Chem. 11*, 2344−2349.

(19) Rauch, M. E., Ferguson, C. G., Prestwich, G. D., and Cafiso, D. S. (2002) Myristoylated alanine-rich C kinase substrate (MARCKS) sequesters spin-labeled phosphatidylinositol 4,5-bisphosphate in lipid bilayers. *J. Biol. Chem. 277*, 14068−14076.

(20) Frazier, A. A., Wisner, M. A., Malmberg, N. J., Victor, K. G., Fanucci, G. E., Nalefski, E. A., Falke, J. J., and Cafiso, D. S. (2002) Membrane orientation and position of the C2 domain from cPLA2 by site-directed spin labeling. *Biochemistry 41*, 6282−6292.

(21) Kohout, S. C., Corbalan-Garcia, S., Gomez-Fernandez, J. C., and Falke, J. J. (2003) C2 domain of protein kinase C α: Elucidation of the membrane docking surface by site-directed fluorescence and spin labeling. *Biochemistry 42*, 1254−1265.

(22) Klug, C. S., Su, W., and Feix, J. B. (1997) Mapping of the residues involved in a proposed β-strand located in the ferric enterobactin receptor FepA using site-directed spin-labeling. *Biochemistry 36*, 13027−13033.

(23) Dalton, L. A., Mcintyre, J. O., and Fleischer, S. (1987) Distance Estimate of the Active-Center of D-β-Hydroxybutyrate Dehydrogenase from the Membrane Surface. *Biochemistry 26*, 2117−2130.

(24) Tapper, A. R., and George, A. L. Jr. (2000) MinK subdomains that mediate modulation of and association with KvLQT1. *J. Gen. Physiol. 116*, 379−390.

(25) Anantharam, A., Lewis, A., Panaghie, G., Gordon, E., McCrossan, Z. A., Lerner, D. J., and Abbott, G. W. (2003) RNA interference reveals that endogenous *Xenopus* MinK-related peptides govern mammalian K^+ channel function in oocyte expression studies. *J. Biol. Chem. 278*, 11739−11745.

(26) Whitmore, L., and Wallace, B. A. (2008) Protein secondary structure analyses from circular dichroism spectroscopy: Methods and reference databases. *Biopolymers 89*, 392−400.

(27) Sreerama, N., Venyaminov, S. Y., and Woody, R. W. (1999) Estimation of the number of α-helical and β-strand segments in proteins using CD spectroscopy. *Biophys. J. 76*, A381.

(28) van Stokkum, I. H., Spoelder, H. J., Bloemendal, M., van Grondelle, R., and Groen, F. C. (1990) Estimation of protein secondary structure and error analysis from circular dichroism spectra. *Anal. Biochem. 191*, 110−118.

(29) Provencher, S. W., and Glockner, J. (1981) Estimation of globular protein secondary structure from circular dichroism. *Biochemistry 20*, 33−37.

(30) Gennis, R. B. (1989) *Biomembranes: Molecular Structure and Function*, Springe-Verlag, New York.

(31) Pohl, T., Spatzal, T., Aksoyoglu, M., Schleicher, E., Rostas, A. M., Lay, H., Glessner, U., Boudon, C., Hellwig, P., Weber, S., and Friedrich, T. (2010) Spin labeling of the *Escherichia coli* NADH ubiquinone oxidoreductase (complex I). *Biochim. Biophys. Acta 1797*, 1894−1900.

(32) Naber, N., Rice, S., Matuska, M., Vale, R. D., Cooke, R., and Pate, E. (2003) EPR spectroscopy shows a microtubule-dependent conformational change in the kinesin switch 1 domain. *Biophys. J. 84*, 3190−3196.

(33) Glasgow, B. J., Gasymov, O. K., Abduragimov, A. R., Yusifov, T. N., Altenbach, C., and Hubbell, W. L. (1999) Side chain mobility and ligand interactions of the G strand of tear lipocalins by site-directed spin labeling. *Biochemistry 38*, 13707−13716.
(34) Fanucci, G. E., Cadieux, N., Piedmont, C. A., Kadner, R. J., and Cafiso, D. S. (2002) Structure and dynamics of the β-barrel of the membrane transporter BtuB by site-directed spin labeling. *Biochemistry 41*, 11543−11551.
(35) Horvath, L. I., Knowles, P. F., Kovachev, P., Findlay, J. B. C., and Marsh, D. (1997) A single-residue deletion alters the lipid selectivity of a K^+ channel-associated peptide in the β-conformation: Spin label electron spin resonance studies. *Biophys. J. 73*, 2588−2594.
(36) Aggeli, A., Bannister, M. L., Bell, M., Boden, N., Findlay, J. B. C., Hunter, M., Knowles, P. F., and Yang, J. C. (1998) Conformation and ion-channeling activity of a 27-residue peptide modeled on the single-transmembrane segment of the IsK (minK) protein. *Biochemistry 37*, 8121−8131.
(37) Mercer, E. A. J., Abbott, G. W., Brazier, S. P., Ramesh, B., Haris, P. I., and Srai, S. K. S. (1997) Synthetic putative transmembrane region of minimal potassium channel protein (minK) adopts an α-helical conformation in phospholipid membranes. *Biochem. J. 325*, 475−479.
(38) Rocheleau, J. M., Gage, S. D., and Kobertz, W. R. (2006) Secondary structure of a KCNE cytoplasmic domain. *J. Gen. Physiol. 128*, 721−729.
(39) Lvov, A., Gage, S. D., Berrios, V. M., and Kobertz, W. R. (2010) Identification of a protein-protein interaction between KCNE1 and the activation gate machinery of KCNQ1. *J. Gen. Physiol. 135*, 607−618.